

Atmos. Chem. Phys., 12, 7955–7960, 2012
www.atmos-chem-phys.net/12/7955/2012/
doi:10.5194/acp-12-7955-2012
© Author(s) 2012. CC Attribution 3.0 License.



Evaluation of the absolute regional temperature potential

D. T. Shindell

NASA Goddard Institute for Space Studies and Columbia Earth Institute, New York, NY, USA

Correspondence to: D. T. Shindell (drew.t.shindell@nasa.gov)

Received: 16 March 2012 – Published in Atmos. Chem. Phys. Discuss.: 5 June 2012

Revised: 16 August 2012 – Accepted: 16 August 2012 – Published: 6 September 2012

Abstract. The Absolute Regional Temperature Potential (ARTP) is one of the few climate metrics that provides estimates of impacts at a sub-global scale. The ARTP presented here gives the time-dependent temperature response in four latitude bands (90–28° S, 28° S–28° N, 28–60° N and 60–90° N) as a function of emissions based on the forcing in those bands caused by the emissions. It is based on a large set of simulations performed with a single atmosphere-ocean climate model to derive regional forcing/response relationships. Here I evaluate the robustness of those relationships using the forcing/response portion of the ARTP to estimate regional temperature responses to the historic aerosol forcing in three independent climate models. These ARTP results are in good accord with the actual responses in those models. Nearly all ARTP estimates fall within $\pm 20\%$ of the actual responses, though there are some exceptions for 90–28° S and the Arctic, and in the latter the ARTP may vary with forcing agent. However, for the tropics and the Northern Hemisphere mid-latitudes in particular, the $\pm 20\%$ range appears to be roughly consistent with the 95% confidence interval. Land areas within these two bands respond 39–45% and 9–39% more than the latitude band as a whole. The ARTP, presented here in a slightly revised form, thus appears to provide a relatively robust estimate for the responses of large-scale latitude bands and land areas within those bands to inhomogeneous radiative forcing and thus potentially to emissions as well. Hence this metric could allow rapid evaluation of the effects of emissions policies at a finer scale than global metrics without requiring use of a full climate model.

1 Introduction

The ARTP is an emission metric that provides estimates of regional surface temperature responses to emissions account-

ing for the regional radiative forcings (RFs) caused by the emissions. The ARTP is an analogue of the absolute global temperature potential (AGTP), which provides an estimate of the global mean temperature response to a given emission based on that emission's global mean RF as a function of time (Shine et al., 2005b). Emission metrics such as these are widely used in analysis of the temperature impacts of emission scenarios or mitigation policies and in emissions trading systems. Any of these metrics can be expressed in absolute terms (e.g. ARTP, AGTP) or relative to the value for a reference gas, typically CO₂ (e.g. RTP, GTP).

The ARTP was developed in Shindell and Faluvegi (2010) based on simulations examining the response to RF localized in latitude bands in a full coupled atmosphere-ocean climate model (Shindell and Faluvegi, 2009). The ARTP does not provide temperature change estimates at the small spatial scales required for many impact assessments, but does provide additional insight into the spatial pattern of temperature response to inhomogeneous forcings beyond that available from traditional global metrics. Very few metrics have attempted to examine sub-global scales thus far, though some have used local information with non-linear global damage metrics (Shine et al., 2005a; Lund et al., 2012).

The previous work presented a matrix of forcing/response relationships derived from the GISS climate model and described the ARTP methodology. While uncertainties were characterized for that model (Shindell and Faluvegi, 2009), that provides no information as to how consistent the regional forcing/response relationships are across models. Here I present an evaluation of the robustness of the forcing/response relationships used in the ARTP based on independent climate models. I also document minor corrections and improvements to the methodology and a small extension to the ARTP method to allow estimates of land-area temperature changes.

2 ARTP definition

The $\text{ARTP}_{a,r}(t)$ represents the surface temperature change in area a between time 0 and time t in response to emissions in region r and is defined by:

$$\text{ARTP}_{a,r}(t) = \int_0^t \left(\sum_{a'} (F_{a'}(t')/E_r) \cdot ((dT_a/F_{a'})/(dT(\text{global}F)/F_{\text{global}})) \cdot \text{IRF}(t-t')dt' \right)$$

where the sum is over all areas of the Earth a' , the first term in the sum is the RF in area a' due to unit emissions in area r , the second term in the sum is the dimensionless coefficient giving equilibrium temperature response in area a to forcing in area a' relative to the global mean equilibrium temperature response to globally quasi-uniform forcing, and the IRF is an impulse response function describing the inertial response of global mean surface temperature to globally quasi-uniform forcing in K per W m^{-2} . The forcing per unit emission term is a single timeseries for emissions from any location for well-mixed greenhouse gases (WMOGHGs), but for short-lived compounds this will depend on the location and timing of emissions (Berntsen et al., 2005; Bond et al., 2011; Naik et al., 2007). Recent studies have provided estimates of this term for short-lived species, including (Bond et al., 2011) and (Henze et al., 2012). The second term in the sum is a matrix hereafter called the RTP coefficients and abbreviated $\text{RTPcoeff}_{a',a}$ where a' and a indicate the forcing and response areas, respectively. Evaluation of the robustness of a set of these coefficients is a primary aim of this paper. These coefficients can be used with estimates of forcing per unit regional emission, or alternatively a model such as a chemistry-transport model or chemistry-climate model can be used to calculate forcing. In the former case the ARTP is an emission-metric, while in the latter case the RTP coefficients are used to provide an estimate of the temperature response to a given forcing pattern without the expense of running a full climate model.

As with the other metrics, the $\text{ARTP}_{a,r}$ can be normalized to yield RTP by dividing by the ARTP_a for a 1 kg emission pulse of CO_2 . Hence the $\text{RTP}_{a,r}$ gives the surface temperature response in area a to 1 kg emission in area r relative to the temperature response in area a to 1 kg CO_2 emissions. The relationship between $\text{RTP}_{a,r}$ and GTP_r is:

$$\text{RTP}_{a,r} = \text{GTP}_r \cdot \left(\sum_{a'} (F_{a'} \cdot \text{RTPcoeff}_{a',a}) \right) / F_{\text{global}}$$

where forcings F are per unit emission in area r .

The ARTP can in principle be established for division of the Earth's surface into an arbitrary number of regions. At present, it has been developed for four latitude bands: the Southern Hemisphere extratropics (90°S – 28°S ; SHext), the tropics (28°S – 28°N), the Northern Hemisphere mid-latitudes (28°N – 60°N ; NHml) and the Arctic (60°N – 90°N). In

Table 1. RTP coefficients (unitless regional response per W m^{-2} forcing in the indicated area relative to global sensitivity).

Forcing region	SHext	Tropics	NHml	Arctic	Global
Response region					
SHext	0.38	0.02	0.05	0.00	0.74
Tropics	0.19	0.51	0.15	0.08	1.03
NHml	0.11	0.55	0.49	0.16	1.06
Arctic	0.14	0.36	0.43	0.77	1.58

Global sensitivity is defined here as global mean temperature response per W m^{-2} global quasi-uniform forcing, making the RTP coefficients dimensionless. Values are derived from responses to sulfate, except for SHext and global forcing, for which CO_2 forcing was used (Shindell and Faluvegi, 2009). Note that regional responses to global forcing are provided for comparison and are not used in any of the ARTP calculations presented here.

this realization it thus becomes:

$$\begin{aligned} \text{ARTP}_{a,r}(t) = & \int_0^t (\text{RTPcoeff}_{\text{SHext},a} \cdot F_{\text{SHext}}(t')/E_r \\ & + \text{RTPcoeff}_{\text{Tropics},a} \cdot F_{\text{Tropics}}(t')/E_r + \text{RTPcoeff}_{\text{NHml},a} \\ & \cdot F_{\text{NHml}}(t')/E_r + \text{RTPcoeff}_{\text{Arctic},a} \cdot F_{\text{Arctic}}(t')/E_r) \cdot \text{IRF}(t-t')dt' \end{aligned}$$

where F_{area}/E_r is the RF in the given area per unit emission in area r and the RTP coefficients are given in Table 1. In the cases examined in the remainder of this paper, a forcing pattern is taken as the starting point for the analysis and so the goal is to evaluate the temperature response to that forcing. In that case, using the forcing/response portion of the ARTP metric, the relevant equation is:

$$\begin{aligned} dT_a(t) = & \int_0^t (\text{RTPcoeff}_{\text{SHext},a} \cdot F_{\text{SHext}}(t') + \text{RTPcoeff}_{\text{Tropics},a} \\ & \cdot F_{\text{Tropics}}(t') + \text{RTPcoeff}_{\text{NHml},a} \cdot F_{\text{NHml}}(t') + \text{RTPcoeff}_{\text{Arctic},a} \\ & \cdot F_{\text{Arctic}}(t')) \cdot \text{IRF}(t-t')dt' \end{aligned}$$

The IRF can be defined as:

$$f(t) = 0.631/8.4 \exp(-t/8.4) + 0.429/409.5 \exp(-t/409.5)$$

where t is the time in years and the two exponentials approximate the relatively rapid response of the land and upper ocean and the slower response of the deep ocean as reported for simulations with the Hadley Centre climate model (Boucher and Reddy, 2008). The sum of the first coefficients in each term, 0.631 and 0.429, gives the approximate equilibrium climate sensitivity assumed in the limit of long times ($1.06\text{ C per } \text{W m}^{-2}$; corresponding to 3.9 C for a doubling of CO_2). The approximate equilibrium temperature response to constant forcing in a model or for a chosen climate sensitivity is simply the sum of RTP coefficient-weighted regional RFs multiplied by the equilibrium climate sensitivity:

$$dT_a = (\text{RTPcoeff}_{\text{SHext},a} \cdot F_{\text{SHext}} + \text{RTPcoeff}_{\text{Tropics},a}$$

$$\cdot F_{\text{Tropics}} + \text{RTPcoeff}_{\text{NHml},a} \cdot F_{\text{NHml}} + \text{RTPcoeff}_{\text{Arctic},a} \cdot F_{\text{Arctic}})$$

(Global-mean sensitivity)

The RTP coefficients have been constructed by weighting the impact of forcing in different locations on the response region relative to the global mean impact of global mean forcing since impulse response functions are given in terms of global mean response to global mean forcing. This explains why the RTP coefficients in Table 1 are based on responses in the GISS model relative to the same model's equilibrium global sensitivity. Compared with Shindell and Faluvegi (2010), this representation normalizes the response per unit forcing by the global mean sensitivity rather than the local temperature response to global forcing ($\text{RTPcoeff}_{\text{Global},a}$). This is a better representation of the regional responses, as the division by $\text{RTPcoeff}_{\text{Global},a}$ values incorrectly removed the regional inhomogeneity in sensitivity seen even for a globally uniform forcing.

Presenting the RTP coefficients in this manner also makes their physical meaning clearer. The global column (Table 1) represents the regional climate sensitivity relative to the global mean. For example, the Arctic response to a globally uniform forcing is 158 % of the global mean response, while the SHext response is only 75 % of the global mean. The regional responses to regional forcings show how much the forcing in each band affects the local area relative to the impact of globally uniform forcing. Hence for a given band, these values indicate how much the local and remote forcings contribute to the climate sensitivity of that band. For example, in the Arctic, roughly half the 158 % Arctic relative sensitivity comes from local Arctic forcing. At Northern Hemisphere mid-latitudes, both tropical and NHml forcing both contribute about 50 % of the response to globally uniform forcing, while the Southern Hemisphere extratropical and Arctic forcings add another 10–15 % to bring the total NHml sensitivity to a value somewhat above 100 % of the global mean sensitivity. Note that the global column values come from separate simulations (of the response to doubled CO_2) from the regional ones and are presented primarily to examine non-linearity. They could also be used to simplify evaluation of the ARTP of WMGHGs, and hence in any calculation of RTP. Comparing the response to global forcing with the sum of the responses to forcings in the four bands indicates that the SHext responses show substantial non-linearity, approximately a factor of two, while the other three regions are fairly linear (8–24 % difference).

Regional responses to different agents were typically statistically indistinguishable for sulfate, black carbon (BC) and ozone. Hence the results presented here use sulfate, as this was the largest forcing and hence has the smallest uncertainty. The only large deviations from the sulfate responses are seen in the Arctic response to Arctic ozone, which is 0.23, and the Arctic response to Arctic BC, which is -0.17 (though the latter includes only the direct RF and neglects the BC albedo forcing, so is an incomplete measure of Arctic

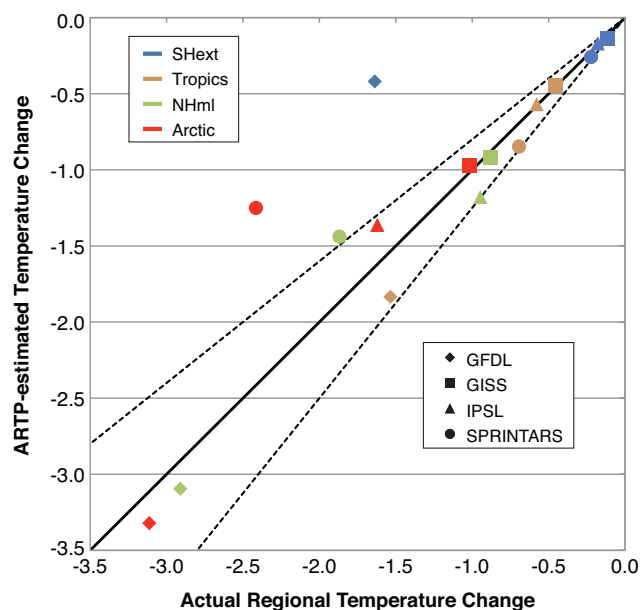


Fig. 1. Regional temperature changes in the indicated models (symbols) and regions (colors) from the actual simulations (horizontal axis) compared with the responses estimated using the forcing/response portion of the ARTP (vertical axis). Dashed lines show $\pm 20\%$ agreement thresholds.

BC's impacts). In cases where ozone and BC forcing diagnostics are available, those coefficients could be used. There is minimal difference between the values presented here for sulfate and the averages presented in Shindell and Faluvegi (2010) for the average of sulfate and idealized CO_2 forcings. I switch to sulfate-only results only as many are uncomfortable with the use of results from idealized CO_2 perturbation experiments (though they were intended to be illustrative only).

The latitude bands used in the ARTP were chosen because there are significant horizontal mixing barriers near these latitudes and hence historical inhomogeneous forcings show large gradients between these bands (e.g. Fig. 1 of (Shindell et al., 2012)). It would be useful to see if robust metrics could be found at smaller spatial scales in both latitude and longitude. Since full coupled model climate response simulations are required to calculate the RTP coefficients, such studies become quite computationally expensive as scales become smaller since this requires both more simulations and often longer simulations to obtain statistically significant results as more localized forcings are reduced in magnitude.

3 Evaluation of multiple climate models

A previous study examined the spatial patterns of radiative forcing and climate response in four coupled atmosphere-ocean climate models driven by historical changes in aerosols (Shindell et al., 2010). Results are analyzed here

from those same simulations, using mixed-layer oceans in the NOAA Geophysical Fluid Dynamics Laboratory (GFDL) (Ming and Ramaswamy, 2009) and University of Tokyo, National Institute for Environmental Studies and Frontier Research Center for Global Change (MIROC/SPRINTARS) (Takemura et al., 2006) models, and with full dynamic oceans in the Institute Pierre Simon Laplace (IPSL) (Dufresne et al., 2005; Hourdin et al., 2006) and NASA Goddard Institute for Space Studies (GISS) (Hansen et al., 2007) models. All models included both direct and indirect aerosol effects (total net RF due to all species, direct plus indirect, is used here), based on each groups' own best estimate of the historical emissions changes as in their simulations in support of the Intergovernmental Panel on Climate Change Fourth Assessment. For those simulations, the IPSL model included reflective aerosols only. Regional forcing values are given in Table 2.

The regional forcings and responses from the IPSL, GFDL and SPRINTARS models can be examined to evaluate the robustness of the GISS-based RTP coefficients. Model simulations were either equilibrium (GFDL and SPRINTARS), or results are linear trends over the full length of transient simulations (IPSL and GISS), so there is no time-dependence. Hence in this analysis, the time-invariant version of the temperature response equation presented above is used (last equation in section 2). The global mean sensitivities (global mean temperature change divided by global mean RF from these simulations) are used for ARTP calculations for each model: 0.90 K per W m^{-2} for GFDL, 0.89 K per W m^{-2} for IPSL, 1.10 K per W m^{-2} for SPRINTARS, and 0.50 K per W m^{-2} for GISS. Aside from the GISS model, these values are similar to the 1.06 K per W m^{-2} long-term response embodied in the IRF based on the Hadley Centre model in the time-varying ARTP. The GISS coupled ocean-atmosphere model shows a long-term equilibrium response to CO_2 of 0.7 K per W m^{-2} . The historical transient analyzed here and in the runs from which the RTP coefficients were 120 yr long, so that $\sim 70\%$ of the equilibrium response was realized, leading to the sensitivity of 0.5 K per W m^{-2} . The value is the same for global CO_2 or sulfate forcing, and is virtually identical for the historical transient and 120-yr equilibrium runs, and hence this is the appropriate global mean sensitivity for the GISS model. The full equilibrium response corresponds to a sensitivity of 2.9 K to doubled CO_2 , substantially less than the Hadley Centre coupled model's sensitivity but well within the empirical range. For the IPSL model, as for the GISS model, in effect the transient sensitivity is used rather than the equilibrium sensitivity as this is more applicable to the available experiments. Full time histories of forcing are unavailable, preventing use of the time-dependent ARTP.

Comparison of the results using the forcing/response portion of the ARTP with the actual responses in the three independent models climate simulations shows that they are in general in very good agreement (Fig. 1). The overall correlation of the regional values from the three models is $r^2 = 0.75$,

Table 2. Historical aerosol forcing (W m^{-2}) from the climate models input to the temperature response estimates using the forcing/response portion of the ARTP.

Forcing region	SHext	Tropics	NHml	Arctic
Climate model				
GFDL	-0.49	-2.51	-3.53	-1.57
GISS	-0.28	-0.79	-2.60	-0.68
IPSL	-0.14	-0.55	-1.79	-0.71
SPRINTARS	-0.31	-0.93	-1.51	-0.15

Values are area-weighted averages within the given latitude bands.

and nearly all points lie within 20% of the ARTP estimates. Thus the RTP coefficients derived with the GISS model seem fairly robust, and their use captures most of the regional variations in the three independent climate models. The GISS model results from a historical all-aerosol forcing simulation are shown as well, though these are of course not an independent test as they are from the same model used to derive the RTP coefficients. However, they do indicate that the RTP coefficients derived from idealized equilibrium simulations provide a good estimate of the actual response to realistic temporally and spatially varying forcing. Note that as the historical forcings were primarily located at NHml and the tropics, and responses are largely in those two regions and the Arctic, this analysis provides the strongest test of the six RTP coefficients relating these areas (the last three rows of the tropics and NHml columns in Table 1). Additional simulations would be required to better evaluate the other 10 coefficients.

Two points stand out as different in Fig. 1, with the calculations using the forcing/response portion of the ARTP substantially underestimating the actual response in the SHext for GFDL and in the Arctic for SPRINTARS. The latter could result from either a larger polar amplification in SPRINTARS than in the other models or from a weaker impact of BC in the Arctic than the use of the sulfate-based RTP coefficients implicitly assumes. For the SHext case, as discussed previously there is a large non-linearity in the SHext responses so that the sum of responses to forcing in each region is only about half the response to global mean forcing. Thus the underestimate in the GFDL model may reflect the relatively weak response in this region in the GISS localized forcing experiments, although the SHext ARTP-based temperature estimates agree well with the actual response for the IPSL and SPRINTARS models. Note that both points with large biases occur in areas with comparatively little forcing (Table 2), and are thus highly sensitive to non-diagonal terms in the RTP coefficient matrix, and in mixed-layer ocean models. Thus these biases could well reflect the lack of dynamic ocean responses that affect these areas. Analysis of additional dynamic ocean-atmosphere models would help clarify the robustness of the Arctic and SHext responses. As the

ARTP-based results for the tropics and NHml are all within $\pm 20\%$ of the actual responses, it seems appropriate to consider 20% to be the approximate 95% confidence interval. For the Arctic and SHext cases, 20% seems to be more representative of the 1-sigma confidence interval ($\sim 66\%$).

4 Extension of ARTP to land area response

I have also examined the ratio of temperature change over land areas within a band to the temperature change of the band as a whole. Land areas are known to respond more strongly to forcing both due to reduced heat capacity relative to the oceans that allows more rapid responses and to limitations in evaporation over land relative to ocean (Meehl et al., 2007; Joshi et al., 2008). Hence these ratios would be expected to generally be greater than one for the temperature response induced by historic aerosol changes (especially in the transient simulations). The multi-model analysis allows precise quantification of this ratio and determination of its robustness. I find that tropical land areas respond 39–45% more than the entire tropics, and NHml land areas change 9–39% more than the NHml band as a whole (where the range is the full spread across the four models). Enhancement for land areas in the Arctic and the SHext are not consistent in sign across models. Thus in the tropics and NHml, where the ratio is relatively robust across the models (despite their differing configurations), multiplication of the temperature estimates using the forcing/response portion of the ARTP for the tropics and NHml by the median enhancements, 1.42 and 1.24, respectively, can provide a useful projection of land area temperatures while adding uncertainty that is small (tropics) or comparable (NHml) to that from the RTP coefficients.

5 Discussion and conclusion

This paper presents a revised ARTP emission metric for estimating the regional temperature response to emissions leading to either homogeneous or inhomogeneous forcing. Evaluation of the forcing/response portion of the ARTP applied to forcing from three independent climate models shows that the metric generally provides a good estimate of latitude band temperature responses, with a particularly narrow uncertainty range of $\sim 20\%$ (95% confidence) in the tropics and the NH mid-latitudes. In those regions, ARTP-based estimates of land area responses can be obtained by multiplying the values by 1.42 and 1.24, respectively, with corresponding uncertainties of 20% and 25% (adding the uncertainties from the RTP coefficient and the land-area enhancement in quadrature). Hence the forcing/response portion of the ARTP appears to provide a useful method for evaluation of large-area temperature responses.

As described previously, the historical aerosol forcing experiments used here provide a good test of many of the RTP

coefficients, but owing to the forcing having been mostly in the tropical and NHml they do not constrain the coefficients for forcing located in the SHext or Arctic as well. Analysis of simulations with substantial forcing at those latitudes, or alternatively direct calculation of the RTP coefficients in other climate models, would provide valuable insight into the robustness of the remaining coefficients.

There is uncertainty in the forcing attributable to emissions, which would contribute to uncertainty in the full ARTP emission metric values. Analysis of intermodel variations suggests that for many short-lived species these are significant (e.g. Fuglestedt et al., 2010). These uncertainties are applicable to all emission metrics, however, including GTP or global warming potential. Hence the uncertainty ranges found here for the forcing/response portion of the ARTP and $ARTP_{land}$ represent the additional uncertainty moving from a global to a regional emission metric rather than the total uncertainty for the emission metric.

There is of course also uncertainty in the climate response function. In the time-varying ARTP, depending on the rate of ocean heat uptake and the complexity of the processes (e.g. carbon cycling) included in the temperature response calculation, the IRF can vary substantially (Gillett and Matthews, 2010; Sarofim, 2011). Though such uncertainty does not affect the temperature change estimated here using the forcing/response portion of the ARTP, as those calculations used the actual modeled global mean sensitivity rather than an impulse response function, such uncertainty needs to be included in temperature estimates based on the ARTP (or other metrics) that use the IRF. In the time-invariant version, the uncertainty in the temperature response at a point in time (e.g. equilibrium) could be characterized by including uncertainty in global mean climate sensitivity. Uncertainty in the IRF would also affect RTP estimates, but generally less so as the IRF appears in both the numerator and the denominator.

While the ARTP metric extends beyond the information provided by global mean metrics, there is clearly a large gap remaining between the spatial scales of information available from the ARTP and that needed for impact assessment. Further work is clearly needed to see how much more regional information can be provided by regional climate metrics, including investigation of impacts beyond temperature. The conclusion presented here that the forcing/response portion of the ARTP appears to be relatively robust across models is an encouraging sign for ongoing efforts to provide sub-global metrics.

Acknowledgements. I thank Greg Faluvegi for assistance with calculations, William Collins at the UK Met Office for pointing out the correction needed to the ARTP definition given previously, the other three modeling groups for providing data for the earlier paper, and NASA's Modeling and Analysis Program for funding. I also thank the two anonymous reviewers as well as William Collins and Glen Peters for their helpful comments.

Edited by: T. Butler

References

- Berntsen, T. K., Fuglestedt, J. S., Joshi, M. M., Shine, K. P., Stuber, N., Ponater, M., Sausen, R., Hauglustaine, D. A., and Li, L.: Response of climate to regional emissions of ozone precursors: sensitivities and warming potentials, *Tellus B – Chem. Phys. Meteorol.*, *57*, 283–304, 2005.
- Bond, T., Zarzycki, C., Flanner, M., and Koch, D.: Quantifying immediate radiative forcing by black carbon and organic matter with the Specific Forcing Pulse, *Atmos. Chem. Phys.*, *11*, 1505–1525, doi:10.5194/acp-11-1505-2011, 2011.
- Boucher, O. and Reddy, M. S.: Climate trade-off between black carbon and carbon dioxide emissions, *Energy Policy*, *36*, 193–200, 2008.
- Dufresne, J.-L., Quaas, J., Boucher, O., Denvil, S., and Fairhead, L.: Contrasts in the effects on climate of anthropogenic sulfate aerosols between the 20th and the 21st century, *Geophys. Res. Lett.*, *32*, L21703, doi:10.1029/2005GL023619, 2005.
- Fuglestedt, J. S., Shine, K. P., Berntsen, T., Cook, J., Lee, D. S., Stenke, A., Skeie, R. B., Velders, G. J. M., and Waitz, I. A.: Transport impacts on atmosphere and climate: Metrics, *Atmos. Environ.*, *44*, 4648–4677, 2010.
- Gillett, N. and Matthews, H.: Accounting for carbon cycle feedbacks in a comparison of the global warming effects of greenhouse gases, *Environ. Res. Lett.*, *5*, 034011, doi:10.1088/1748-9326/5/3/034011, 2010.
- Hansen, J., Sato, M., Ruedy, R., Kharecha, P., Lacis, A., Miller, R. L., Nazarenko, L., Lo, K., Schmidt, G. A., Russell, G., Aleinov, I., Bauer, S., Baum, E., Cairns, B., Canuto, V., Chandler, M., Cheng, Y., Cohen, A., Genio, A. D., Faluvegi, G., Fleming, E., Friend, A., Hall, T., Jackman, C., Jonas, J., Kelley, M., Kiang, N. Y., Koch, D., Labow, G., Lerner, J., Menon, S., Novakov, T., Oinas, V., Perlwitz, J., Perlwitz, J., Rind, D., Romanou, A., Schmunk, R., Shindell, D., Stone, P., Sun, S., Streets, D., Tausnev, N., Thresher, D., Unger, N., Yao, M., and Zhang, S.: Climate simulations for 1880–2003 with GISS modelE, *Clim. Dynam.*, *29*, 661–696, 2007.
- Henze, D. K., Shindell, D. T., Akhtar, F., Spurr, R. J. D., Pinder, R. W., Loughlin, D., Kopacz, M., Singh, K., and Shim, C.: Spatially refined aerosol direct radiative forcing efficiencies, submitted to *Environ. Sci. Tech.*, 2012.
- Hourdin, F., Musat, I., Bony, S., Braconnot, P., Codron, F., Dufresne, J.-L., Fairhead, L., Filiberti, M.-A., Friedlingstein, P., Grandpeix, J.-Y., Krinner, G., Levan, P., Li, Z.-X., and Lott, F.: The LMDZ4 general circulation model: climate performance and sensitivity to parametrized physics with emphasis on tropical convection, *Clim. Dynam.*, *27*, 787–813, 2006.
- Joshi, M., Gregory, J., Webb, M., Sexton, D., and Johns, T.: Mechanisms for the land/sea warming contrast exhibited by simulations of climate change, *Clim. Dynam.*, *30*, 455–465, doi:10.1007/s00382-007-0306-1, 2008.
- Lund, M., Berntsen, T., Fuglestedt, J., Ponater, M., and Shine, K.: How much information is lost by using global-mean climate metrics? an example using the transport sector, *Clim. Change*, *113*, 949–963, doi:10.1007/s10584-011-0391-3, 2012.
- Meehl, G. A., Stocker, T. F., Collins, W. D., Friedlingstein, P., Gaye, A. T., Gregory, J. M., Kitoh, A., Knutti, R., Murphy, J. M., Noda, A., Raper, S. C. B., Watterson, I. G., Weaver, A. J., and Zhao, Z.-C.: Global Climate Projections, in: *Climate Change 2007: The Physical Science Basis. Contribution of Working Group I to the Fourth Assessment Report of the Intergovernmental Panel on Climate Change*, edited by: Solomon, S., Qin, D., Manning, M., Chen, Z., Marquis, M., Averyt, K. B., Tignor, M., and Miller, H. L., Cambridge Univ. Press, Cambridge, UK and New York, NY, USA, 2007.
- Ming, Y. and Ramaswamy, V.: Nonlinear Climate and Hydrological Responses to Aerosol Effects, *J. Climate*, *22*, 1329–1339, doi:10.1175/2008jcli2362.1, 2009.
- Naik, V., Mauzerall, D. L., Horowitz, L. W., Schwarzkopf, M. D., Ramaswamy, V., and Oppenheimer, M.: On the sensitivity of radiative forcing from biomass burning aerosols and ozone to emission location, *Geophys. Res. Lett.*, *34*, L03818, doi:10.1029/2006gl028149, 2007.
- Sarofim, M. C.: The GTP of Methane: Modeling Analysis of Temperature Impacts of Methane and Carbon Dioxide Reductions, *Environ. Model Assess.*, *17*, 231–239, 2011.
- Shindell, D. and Faluvegi, G.: Climate response to regional radiative forcing during the twentieth century, *Nature Geosci.*, *2*, 294–300, doi:10.1038/ngeo473, 2009.
- Shindell, D. and Faluvegi, G.: The net climate impact of coal-fired power plant emissions, *Atmos. Chem. Phys.*, *10*, 3247–3260, doi:10.5194/acp-10-3247-2010, 2010.
- Shindell, D., Schulz, M., Ming, Y., Takemura, T., Faluvegi, G., and Ramaswamy, V.: Spatial scales of climate response to inhomogeneous radiative forcing, *J. Geophys. Res.-Atmos.*, *115*, D19110, doi:10.1029/2010jd014108, 2010.
- Shindell, D. T., Voulgarakis, A., Faluvegi, G., and Milly, G.: Precipitation response to regional radiative forcing, *Atmos. Chem. Phys.*, *12*, 6969–6982, 2012, <http://www.atmos-chem-phys.net/12/6969/2012/>.
- Shine, K. P., Berntsen, T. K., Fuglestedt, J. S., and Sausen, R.: Scientific issues in the design of metrics for inclusion of oxides of nitrogen in global climate agreements, *Proc. Natl. Acad. Sci.*, *102*, 15768–15773, 2005a.
- Shine, K. P., Fuglestedt, J. S., Hailemariam, K., and Stuber, N.: Alternatives to the Global Warming Potential for Comparing Climate Impacts of Emissions of Greenhouse Gases, *Clim. Change*, *68*, 281–302, 2005b.
- Takemura, T., Tsushima, Y., Yokohata, T., Nozawa, T., Nagashima, T., and Nakajima, T.: Time evolutions of various radiative forcings for the past 150 years estimated by a general circulation model, *Geophys. Res. Lett.*, *33*, L19705, doi:10.1029/2006GL026666, 2006.